1 **Distinct roles of prefrontal cortex neurons in set shifting**
2
3 Marco Nigro [1] [*], Lucas Silva Tortorelli [1] [*] and Hongdian Yang [1,2]
4
5 [1] Department of Molecular, Cell and Systems Biology, [2] Neuroscience Graduate Program,
6 University of California, Riverside, CA 92521, USA
7
8 [*] Equal contributions
9
10 Correspondence: hongdian@ucr.edu
11
12
13 **Abstract**
14
15 Cognitive flexibility, the ability to adjust behavioral strategies in response to changing
16 environmental contingencies, requires adaptive processing of internal states and contextual cues
17 to guide goal-oriented behavior, and is dependent on prefrontal cortex (PFC) functions. However,
18 the neurophysiological underpinning of how the PFC supports cognitive flexibility is not well
19 understood and has been under active investigation. We recorded spiking activity from single
20 PFC neurons in mice performing the attentional set-shifting task, where mice learned to associate
21 different contextually relevant sensory stimuli to reward. We identified subgroups of PFC neurons
22 encoding task context, choice and trial outcome. Putative fast-spiking neurons were more
23 involved in representing outcome and choice than putative regular-spiking neurons. Regression
24 model further revealed that task context and trial outcome modulated the activity of choice-
25 encoding neurons in rule-dependent and cell type-dependent manners. Together, our data
26 provide new evidence to elucidate PFC's role in cognitive flexibility, suggesting differential cell
27 type-specific engagement during set shifting, and that both contextual rule representation and trial
28 outcome monitoring underlie PFC's unique capacity to support flexible behavioral switching.
29
30 **Introduction**
31
32 The ability to adjust behavioral strategies in response to changing environmental contingencies,
33 termed cognitive flexibility, serves as an essential executive function. Flexibility, or rule switching,
34 requires adaptive processing of internal states and contextual cues to guide goal-oriented
35 behavior, and is vital to the survival of organisms. Inappropriate behavioral adjustments, such as
36 deficits in modifying responses to a rule change, are a hallmark of impaired executive functions
37 observed in a broad spectrum of psychiatric disorders (Miller and Cohen, 2001; Uddin, 2021).
38
39 Considerable efforts have been made to uncover the neural substrates of flexible behavioral
40 switching (see reviews (Mesulam, 1998; Miller, 1999; Miller and Cohen, 2001; Ragozzino, 2007;
41 Le Merre et al., 2021; Uddin, 2021)). Set shifting, a type of rule switching that requires attending
42 to or ignoring a stimulus feature in a context-dependent way, is widely used to assess cognitive
43 flexibility. The Wisconsin Card Sorting Test (WCST), the Intra-Extra Dimensional Set Shift Task
44 (IED) and their analogs have been implemented to test human and animal subjects (Berg, 1948;
45 Milner, 1963; Roberts et al., 1988; Dias et al., 1996a; Monchi et al., 2001; Barnett et al., 2010;
46 Brown and Tait, 2015). Decades of research have established that the prefrontal cortex (PFC) is
47 required for set shifting (Berg, 1948; Milner, 1963; Dias et al., 1996a, 1996b; Ridderinkhof, 2004;
48 Ragozzino, 2007; Floresco et al., 2009; Dajani et al., 2020). However, the neurophysiological
49 underpinning of how the PFC mediates different aspects of flexible decision-making processes to
50 support set shifting is not well understood. Importantly, although loss-of-function work has shown
51 that the medial PFC (mPFC) is associated with attentional switching across, but not within

52 perceptual dimensions (e.g., (Owen et al., 1991; Dias et al., 1996b, 1997; Birrell and Brown, 2000;
53 Ridderinkhof, 2004; Ragozzino, 2007; Bissonette et al., 2008)), the neural substrates that support
54 such functional specificity remain elusive and are under active investigation (e.g., (Cho et al.,
55 2020, 2023; Benoit et al., 2022)).
56
57 In an effort to advance our understanding of PFC's role in flexible behavior, we trained mice to
58 perform the attentional set-shifting task (AST), which follows the principles of WCST and IED, and
59 trains animals to continuously adapt to multiple rule changes (Birrell and Brown, 2000; Colacicco
60 et al., 2002; Garner et al., 2006; Bissonette et al., 2008; Lapiz-Bluhm et al., 2008; Heisler et al.,
61 2015) (Fig. 1A). These rule changes may or may not involve the mPFC (Birrell and Brown, 2000;
62 McAlonan and Brown, 2003; Bissonette et al., 2008, 2013). Specifically, in extra-dimensional shift
63 (EDS) subjects learn to attend to a novel stimulus from a different dimension (e.g., from digging
64 medium to odor) to seek reward, and task performance is impaired by mPFC lesion. In contrast,
65 intra-dimensional reversal (REV) requires attending to a previously unrewarding stimulus and
66 ignoring a previously rewarding stimulus within the same stimulus dimension, and is not affected
67 by mPFC lesion.
68
69 We recorded spiking activity from single units in mice performing AST. We identified subgroups
70 of mPFC neurons representing different task-related variables, namely task context, trial outcome
71 and choice. We found that putative fast-spiking neurons were more engaged in representing
72 outcome and choice than putative regular-spiking neurons. We showed that both context and
73 outcome signals significantly modulated the activity of choice-encoding neurons in EDS. The
74 modulatory effects were most obvious in fast-spiking neurons and were absent in REV. Together,
75 our data suggest differential cell type-specific engagement during rule switching, and that both
76 contextual rule representation and outcome monitoring underlie mPFC's unique role in supporting
77 set-shifting behavior.
78
79 **Results**
80
81 We trained mice to perform the attentional set-shifting task (AST) using procedures similar to
82 previous work (Methods. Liston et al., 2006; Snyder et al., 2012). Briefly, in most stages of the
83 task, mice learned to associate one relevant sensory stimulus out of several possible ones to
84 reward (Fig. 1A, Fig. S1). The relevant stimulus remained in the dimension of digging medium in
85 early stages of the task (simple discrimination, SD; compound discrimination, CD; intra-
86 dimensional reversal, REV; intra-dimensional shift, IDS), and shifted to the dimension of odor in
87 the last stage of extra-dimensional shift (EDS). Mice promptly learned to follow the rule in each
88 stage. However, REV and EDS appeared to be more challenging as mice needed more trials to
89 reach performance criterion (six consecutive correct trials, Fig. 1B) (Birrell and Brown, 2000;
90 Liston et al., 2006; Snyder et al., 2012). To elucidate the role of mPFC in cognitive flexibility, we
91 conducted tetrode recording during task performance (161 single units from 15 sessions, Fig. 1C-
92 E, Methods). Previous loss-of-function studies have reported that the mPFC is specifically
93 required for the successful completion of EDS (e.g., (Dias et al., 1996b; Birrell and Brown, 2000;
94 Bissonette et al., 2008)), and our analyses were focused on EDS to assess the neural substrates.
95
96 First, we sought out to examine the extent to which abstract contextual rule information was
97 represented in the mPFC. In AST, this refers to the stimulus dimension that subjects learn to
98 attend to (digging medium vs. odor). Plateaued performance following a rule change has been
99 taken as important evidence that subjects readily adapt to the new rule (e.g., (Mansouri et al.,
100 2006; Sleezer et al., 2016)). Indeed, we found that the spiking activity of a subset of mPFC
101 neurons tracked the attended stimulus dimension when performance was plateaued (last set of
102 consecutive correct trials, Fig. 2A, B). Using Receiver-Operating-Characteristic (ROC) analysis

103 (Green and Swets, 1966), we identified 31% (50/161) of mPFC neurons whose activity was
104 significantly correlated with task context (Fig. 2C-G, Methods), and we referred to them as context
105 neurons. Similar numbers of neurons exhibited higher or lower activity when the relevant stimulus
106 dimension shifted from digging medium to odor (context+ vs. context-, 27 vs. 23 neurons). We did
107 not include SD in the analysis because the odor dimension was not explicitly introduced (Fig. 1A,
108 Methods). However, the identified context neurons exhibited comparable activity in SD as in other
109 digging medium-relevant stages (Fig. S2), supporting their robust representation of stimulus
110 dimension. Further, the classification of context neurons was supported by a generalized linear
111 model (GLM), where the coefficients of stimulus dimension were significantly stronger than other
112 task-related variables, and stronger than those of non-context neurons (Fig. S3, Methods). We
113 trained a decoder to evaluate the extent to which we can predict the shift of task context based
114 on context neuron activity, and the decoder was able to achieve 80.8 ± 5.9% accuracy (Fig. 2H,
115 I, Methods). Context-related activity sustained for tens of seconds before explicit task
116 engagement (Fig. S4), suggesting that context information was represented in persistent activity,
117 in support of other studies (e.g., (Mansouri et al., 2006; Sleezer et al., 2016; Bari et al., 2019)).
118 We next evaluated context neuron activity during rule learning and found that their activity
119 exhibited gradual changes when the relevant dimension shifted from digging medium to odor
120 (from IDS to EDS, Fig. 2J, K). Since the dimensional rule shift was not cued, this finding supports
121 that context representation develops over learning.

123 To examine the contributions of different cell types to set shifting, we classified the recorded units
124 into putative inhibitory fast spiking (FS) and putative excitatory regular spiking (RS) based on
125 spike waveform features and firing rate (Barthó et al., 2004; Ji and Neugebauer, 2012): FS, trough
126 to peak = 0.35 ± 0.02 ms; baseline firing rate = 28.14 ± 2.77 spikes/s, n = 19; RS, trough to peak
127 = 0.67 ± 0.01 ms; baseline firing rate = 2.85 ± 0.24 spikes/s, n = 112 (Methods, Fig. 2L). The
128 remaining units were considered unidentified and excluded from cell type-related analyses. We
129 found similar proportions of RS and FS neurons encoding task context (34/112 RS vs. 6/19 FS,
130 30% vs. 32%, p = 0.91, chi-squared test, Fig. 2M).

132 Next, we evaluated to what extent mPFC activity represented previous trial outcome. Using similar
133 ROC analysis, we identified 22% (36/161) of neurons exhibiting differential activity following
134 correct (rewarded) or incorrect (unrewarded) trials (Fig. 3A, B, Methods). 64% of these neurons
135 (23/36) showed higher activity when previous trials were correct compared with when previous
136 trials were incorrect (outcome+, Fig. 3C). The remaining 36% of outcome neurons (13/36)
137 exhibited the opposite trend, increasing firing rate following incorrect trials compared to following
138 correct trials (outcome-, Fig. 3D). Based on outcome neuron activity, a decoder was able to predict
139 trial outcome with 83.0 ± 3.4% accuracy (Fig. 3E, Methods). Similar to context encoding, outcome-
140 related activity sustained for tens of seconds prior to task engagement (Fig. S5), indicating that
141 outcome information (in particular negative outcome) was represented in persistent mPFC activity.
142 28% (10/36) of outcome-encoding neurons also represented context, supporting mixed tuning in
143 the PFC (Rigotti et al., 2013; Fusi et al., 2016; Tye et al., 2024). Interestingly, higher proportions
144 of FS neurons were found to represent outcome (26/112 RS vs. 9/19 FS, 23% vs. 47%, p = 0.028,
145 Fig. 3F).

147 We then identified choice neurons, whose activity correlated with the upcoming choices on current
148 trials (correct vs. incorrect, 23/161, Fig. 4A, B). 56% of these neurons (13/23) exhibited higher
149 activity preceding correct choices than incorrect choices (Fig. 4C). These neurons, hereafter
150 referred to as choice+, also showed significantly elevated activity immediately before correct
151 choices compared to after these choices. In contrast, their activity before and after incorrect
152 choices were similar (Fig. S6A). Choice- neurons (10/23) exhibited lower activity preceding
153 correct choices than incorrect choices (Fig. 4D), and did not show any differential activity before

154 and after correct or incorrect choices (Fig. S6B). A decoder was able to predict trial-by-trial
155 choices with 80.8 ± 2.1% accuracy from choice neuron activity (Fig. 4E, Methods). We also found
156 higher proportion of FS neurons encoding choice (12/112 RS vs. 6/19 FS, 11% vs. 32%, p = 0.015,
157 Fig. 4F). A considerable fraction of choice-encoding neurons also represented other task-related
158 variables (43% (10/23) choice neurons represented outcome, and 39% (9/23) choice neurons
159 also represented context), in further support of mixed tuning. Together, our results showed that
160 putative FS neurons were more involved in representing outcome and choice during set shifting.
161
162 To understand how context and outcome may affect decision making, we examined the impact of
163 these two variables on the activity of choice neurons. We divided each trial into four 2-s bins, with
164 two bins prior to trials start (T1, T2), and two other bins prior to choice (T3, T4. Fig. 5A). We used
165 GLM to calculated the regression coefficients for the regressors of trial outcome and contextual
166 rule on choice neurons in EDS. GLM confirmed that the identified choice+ neurons prominently
167 represented the choice signal prior to digging (Fig. S7). Interestingly, these neurons showed non-
168 zero coefficients for outcome and context. Specifically, we found significant coefficients for
169 outcome before trial start (T1, T2) and before choice (T4, Fig. 5B). For context, we observed
170 significant non-zero coefficients before trial start (T2) and before choice (T3, T4, Fig. 5C). These
171 effects were mostly absent in choice- neurons (Fig. S8). Albeit the small sample sizes, the
172 modulatory effects were present in FS neurons, as choice+ FS neurons exhibited significant
173 coefficients for outcome (T1-T4) and context (T2, Fig. 5D, E). In contrast, choice-encoding RS
174 neurons were not modulated by outcome or context (Fig. 5F, G). In summary, our findings
175 revealed distinct modulation patterns in putative FS and RS neurons, with context and outcome-
176 related information primarily affecting FS activity.
177
178 Lastly, we wondered whether the observed modulation patterns were specific to EDS switching.
179 We analyzed REV as a comparison, which was also behaviorally demanding but not affected by
180 mPFC perturbation (Fig. 1B, Birrell and Brown, 2000; Bissonette et al., 2008). We identified
181 largely distinct groups of neurons encoding outcome and choice in REV (Outcome, REV vs EDS:
182 22 vs. 36 neurons, 4 overlapped neurons; Choice, REV vs EDS: 19 vs. 23 neurons, 4 overlapped
183 neurons). More mPFC neurons encoded outcome in EDS than REV (Outcome, REV vs. EDS, 14%
184 (22/161) vs. 22% (36/161), p = 0.04; Choice, REV vs. EDS, 12% (19/161) vs. 14% (23/161), p =
185 0.51). Regression analysis revealed that trial outcome did not significantly affect the activity of
186 choice neurons in REV (Fig. 6A, Fig. S9). Since REV did not involve a change of stimulus
187 dimension, we treated the result that task context did not affect choice neuron activity in REV as
188 a positive control (Fig. 6B, Fig. S9). Finally, we assessed how different cell types were engaged
189 in REV and EDS. For choice, we found similar proportions of RS neurons in REV and EDS (REV
190 vs. EDS, 15/112 RS vs. 12/112 RS, 13% vs. 11%, p = 0.54). However, REV engaged a lower
191 proportion of FS choice-encoding neurons (REV vs. EDS, 1/19 FS vs. 6/19 FS, 5% vs. 32%, p =
192 0.037, Fig. 6C). Similarly, lower proportions of FS outcome-encoding neurons were identified in
193 REV (REV vs. EDS, 15/112 RS vs. 26/112 RS, 13% vs. 23%, p = 0.057; 0/19 FS vs. 9/19 FS, 0%
194 vs. 47%, p = 5.9e-4, Fig. 6D). Together, our data uncovered substantial differences in mPFC
195 representation during different types of rule switching behavior, such that task context and trial
196 outcome modulated the activity of choice-encoding neurons only in EDS but not REV, and
197 primarily affected FS but not RS neurons.
198
199 **Discussion**
200
201 To elucidate mPFC's role in cognitive flexibility, we recorded spiking activity from single units in
202 mice performing AST. We identified neuronal subgroups encoding different task-related variables,
203 namely task context, trial outcome and choice. Importantly, we showed that putative FS
204 interneurons were more engaged than putative RS neurons in representing outcome and choice.

205 By contrasting neuronal responses in EDS to REV, regression model revealed that context and
206 outcome signals modulated the activity of choice-encoding neurons in task-dependent and cell
207 type-dependent manners. Together, our data suggest differential cell type-specific engagement
208 during flexible rule switching, and that both contextual rule representation and trial outcome
209 monitoring underlie mPFC's unique capacity to support set shifting.
210
211 mPFC has been proposed to support cognitive flexibility by encoding abstract contextual rules
212 (Wallis et al., 2001; Meyers et al., 2008; Rich and Shapiro, 2009; Durstewitz et al., 2010; Hyman
213 et al., 2012; Mante et al., 2013; Rodgers and DeWeese, 2014; Siniscalchi et al., 2016; Rikhye et
214 al., 2018; Reinert et al., 2021), or by encoding feedback signals (Luk and Wallis, 2009; Bissonette
215 and Roesch, 2015; Del Arco et al., 2017; Bari et al., 2019; Norman et al., 2021; Spellman et al.,
216 2021). These two hypotheses are not necessarily exclusive becasue when subjects are unaware
217 of the rule change, they likely utilize more than one stream of information to solve the task
218 (Ridderinkhof, 2004; Rushworth and Behrens, 2008; Mansouri et al., 2009; Bissonette et al., 2013;
219 Uddin, 2021). Indeed, our data show that abstract contextual rule-related information and trial
220 outcome-related information are both represented in persistent activity in the mPFC. It is possible
221 that using novel rather than familiar cues in EDS is important for the formation and utility of
222 stimulus dimension in the mPFC (Birrell and Brown, 2000; Bissonette et al., 2013).
223
224 Our data further suggest the functional specificity of such representations, as context and
225 outcome affected the activity of choice-encoding neurons only in EDS but not REV. Behaviorally,
226 both REV and EDS appear to be more challenging as subjects typically take more trials to reach
227 performance criterion (Birrell and Brown, 2000; Liston et al., 2006; Snyder et al., 2012). However,
228 these two rule changes are thought to involve different cognitive processes as the former is
229 referred to as affective shifting while the later as attentional shifting (Dias et al., 1996b; Floresco
230 et al., 2009; Young et al., 2010). In REV, subjects are challenged to ignore the relevant stimulus
231 from the previous stage, and to attend to a previously ignored stimulus within the same stimulus
232 dimension. In EDS, subjects learn to direct their responses to a novel cue from the previously
233 irrelevant stimulus dimension. According to learning theories, the improved performance in IDS
234 (fewer trials to complete) strongly suggests that mice attend to the stimulus dimensions (digging
235 medium vs. odor), and that solving EDS involves a shift in the attended dimension, rather than
236 purely responding to specific sensory cues (Mackintosh, 1975; Roberts et al., 1988). Notably, the
237 activity of choice-encoding neurons is modulated by context and outcome only in EDS but not
238 REV, suggesting the unique neural substrates underlying mPFC's functional specificity.
239
240 Why did context and outcome only affect choice+ neuron activity? The plateaued performance
241 toward the end of a behavioral session was considered as rule acquisition, while earlier trials were
242 considered as trial-and-error learning (Sleezer et al., 2016, 2017; Nigro et al., 2023). Thus,
243 incorrect choices likely reflect the early rule learning phase, and correct choices likely reflect the
244 late rule acquisition phase. We speculate that the increase in choice+ neuron activity prior to
245 correct choices is therefore correlated with state changes in switching behavior, suggesting that
246 outcome and context signals are important for driving rule switching in EDS.
247
248 Our findings further suggest a critical role for fast-spiking interneurons in set shifting, consistent
249 with prior working demonstrating the importance of PV-mediated synchrony and differential
250 encoding between RS and FS neurons in flexible behavior (Rikhye et al., 2018; Cho et al., 2020,
251 2023; Benoit et al., 2022). The stronger involvement of putative FS neurons implies a key role of
252 inhibitory signaling in shaping information flow and excitation-inhibition balance, important in
253 many neuropsychiatric conditions (e.g., (Rubenstein and Merzenich, 2003; Cho et al., 2015;
254 Canetta et al., 2016; Cardin, 2018; Sohal and Rubenstein, 2019)).
255

256 One limitation of the current study is the relatively low number of simultaneously recorded neurons
257 per behavioral session, which precludes performing comprehensive population-based analysis to
258 better examine network dynamics (as in (Durstewitz et al., 2010; Jercog et al., 2021; Zhou et al.,
259 2021; Richman et al., 2023)). Another limitation is that some cell type-related findings are based
260 on a relatively low number of FS neurons. These limitations can be aided by recording from
261 genetically identified neurons (e.g., (Pi et al., 2013; Pinto and Dan, 2015; Kim et al., 2016)) in
262 future studies. Nevertheless, our single-cell analysis has uncovered new information on how
263 individual neurons encode information during set shifting, elucidating the fundamental building
264 blocks of neuronal computation and information processing.
265
266 Our work contributes to the growing interest in revealing neural mechanisms underlying more
267 natural, ethologically relevant behavior (Parker et al., 2020; Dennis et al., 2021). Admittedly, such
268 behavioral paradigms may not afford the level of task control more commonly seen in restrained,
269 operant paradigms. Nevertheless, the challenge of dissociating movement-related signal from
270 sensory- or decision-related signal is present in not only freely-moving, but also restrained
271 settings (Musall et al., 2019; Steinmetz et al., 2019; Stringer et al., 2019; Zagha et al., 2022).
272 Comprehensive behavioral tracking and motif analysis (e.g., (Wiltschko et al., 2015; Markowitz et
273 al., 2023)) will help to identify whether specific behavioral patterns are associated with rule
274 switching behavior. Ultimately, cognitive processes are not independent from sensory or motor
275 processes. Cognition, perception and action may be implemented in a distributed rather than
276 isolated manner (Cisek and Kalaska, 2010; Parker et al., 2020; Zagha et al., 2022).
277
278
279 **Author contributions**
280 MN, LST and HY planned the project. LST performed experiments. MN and HY analyzed data
281 and wrote the manuscript with assistance from LST.
282
287
288
289
290
291
292
293
294
295
296
297
298
299
300
301
302
303
304

References

Bari BA, Grossman CD, Lubin EE, Rajagopalan AE, Cressy JI, Cohen JY (2019) Stable Representations of Decision Variables for Flexible Behavior. Neuron 103:1–12 Available at: https://doi.org/10.1016/j.neuron.2019.06.001.

Barnett JH, Robbins TW, Leeson VC, Sahakian BJ, Joyce EM, Blackwell AD (2010) Assessing cognitive function in clinical trials of schizophrenia. Neurosci Biobehav Rev 34:1161–1177 Available at: http://dx.doi.org/10.1016/j.neubiorev.2010.01.012.

Barthó P, Hirase H, Monconduit L, Zugaro M, Harris KD, Buzsáki G (2004) Characterization of neocortical principal cells and interneurons by network interactions and extracellular features. J Neurophysiol 92:600–608.

Benoit LJ, Holt ES, Posani L, Fusi S, Harris AZ, Canetta S, Kellendonk C (2022) Adolescent thalamic inhibition leads to long-lasting impairments in prefrontal cortex function. Nat Neurosci 25:714–725.

Berg EA (1948) A simple objective technique for measuring flexibility in thinking. J Gen Psychol 39:15–22.

Birrell JM, Brown VJ (2000) Medial frontal cortex mediates perceptual attentional set shifting in the rat. J Neurosci 20:4320–4324 Available at: http://www.ncbi.nlm.nih.gov/pubmed/10818167.

Bissonette GB, Martins GJ, Franz TM, Harper ES, Schoenbaum G, Powell EM (2008) Double dissociation of the effects of medial and orbital prefrontal cortical lesions on attentional and affective shifts in mice. J Neurosci 28:11124–11130.

Bissonette GB, Powell EM, Roesch MR (2013) Neural structures underlying set-shifting: Roles of medial prefrontal cortex and anterior cingulate cortex. Behav Brain Res 250:91–101 Available at: http://dx.doi.org/10.1016/j.bbr.2013.04.037.

Bissonette GB, Roesch MR (2015) Neural correlates of rules and conflict in medial prefrontal cortex during decision and feedback epochs. Front Behav Neurosci 9:1–14.

Brown VJ, Tait DS (2015) Attentional Set-Shifting Across Species. In, pp 363–395 Available at: http://link.springer.com/10.1007/7854_2015_5002.

Canetta S, Bolkan S, Padilla-Coreano N, Song LJ, Sahn R, Harrison NL, Gordon JA, Brown A, Kellendonk C (2016) Maternal immune activation leads to selective functional deficits in offspring parvalbumin interneurons. Mol Psychiatry 21:956–968.

Cardin JA (2018) Inhibitory Interneurons Regulate Temporal Precision and Correlations in Cortical Circuits. Trends Neurosci 41:689–700 Available at: https://doi.org/10.1016/j.tins.2018.07.015.

Cho KKA, Davidson TJ, Bouvier G, Marshall JD, Schnitzer MJ, Sohal VS (2020) Cross-hemispheric gamma synchrony between prefrontal parvalbumin interneurons supports behavioral adaptation during rule shift learning. Nat Neurosci 23:892–902 Available at: http://dx.doi.org/10.1038/s41593-020-0647-1.

Cho KKA, Hoch R, Lee AT, Patel T, Rubenstein JLR, Sohal VS (2015) Gamma rhythms link prefrontal interneuron dysfunction with cognitive inflexibility in dlx5/6+/- mice. Neuron 85:1332–1343 Available at: http://dx.doi.org/10.1016/j.neuron.2015.02.019.

Cho KKA, Shi J, Phensy AJ, Turner ML, Sohal VS (2023) Long-range inhibition synchronizes and updates prefrontal task activity. Nature 617:548–554.

Cisek P, Kalaska JF (2010) Neural mechanisms for interacting with a world full of action choices. Annu Rev Neurosci 33:269–298.

Colacicco G, Welzl H, Lipp HP, Würbel H (2002) Attentional set-shifting in mice: Modification of a rat paradigm, and evidence for strain-dependent variation. Behav Brain Res 132:95–102.

Dajani DR, Odriozola P, Winters M, Voorhies W, Marcano S, Baez A, Gates KM, Dick AS, Uddin LQ (2020) Measuring cognitive flexibility with the flexible item selection task: From Fmri adaptation to individual Connectome mapping. J Cogn Neurosci 32:1026–1045.

356 Del Arco A, Park J, Wood J, Kim Y, Moghaddam B (2017) Adaptive encoding of outcome
357   prediction by prefrontal cortex ensembles supports behavioral flexibility. J Neurosci
358   37:8363–8373.
359 Dennis EJ, El Hady A, Michaiel A, Clemens A, Tervo DRG, Voigts J, Datta SR, Gowan Tervo
360   DR, Voigts J, Datta SR (2021) Systems Neuroscience of Natural Behaviors in Rodents. J
361   Neurosci 41:911–919 Available at:
362   http://www.jneurosci.org/lookup/doi/10.1523/JNEUROSCI.1877-20.2020.
363 Dias R, Robbins TW, Roberts AC (1996a) Primate analogue of the Wisconsin card sorting test:
364   Effects of excitotoxic lesions of the prefrontal cortex in the marmoset. Behav Neurosci
365   110:872–886 Available at: http://doi.apa.org/getdoi.cfm?doi=10.1037/0735-
366   7044.110.5.872.
367 Dias R, Robbins TW, Roberts AC (1996b) Dissociation in prefrontal cortex of affective and
368   attentional shifts. Nature 380:69–72.
369 Dias R, Robbins TW, Roberts AC (1997) Dissociable Forms of Inhibitory Control within
370   Prefrontal Cortex with an Analog of the Wisconsin Card Sort Test: Restriction to Novel
371   Situations and Independence from "On-Line" Processing. J Neurosci 17:9285–9297
372   Available at: https://www.jneurosci.org/lookup/doi/10.1523/JNEUROSCI.17-23-
373   09285.1997.
374 Durstewitz D, Vittoz NM, Floresco SB, Seamans JK (2010) Abrupt Transitions between
375   Prefrontal Neural Ensemble States Accompany Behavioral Transitions during Rule
376   Learning. Neuron 66:438–448 Available at:
377   http://linkinghub.elsevier.com/retrieve/pii/S0896627310002321.
378 Floresco SB, Zhang Y, Enomoto T (2009) Neural circuits subserving behavioral flexibility and
379   their relevance to schizophrenia. Behav Brain Res 204:396–409.
380 Fusi S, Miller EK, Rigotti M (2016) Why neurons mix: High dimensionality for higher cognition.
381   Curr Opin Neurobiol 37:66–74 Available at: http://dx.doi.org/10.1016/j.conb.2016.01.010.
382 Garner JP, Thogerson CM, Würbel H, Murray JD, Mench JA (2006) Animal neuropsychology:
383   Validation of the Intra-Dimensional Extra-Dimensional set shifting task for mice. Behav
384   Brain Res 173:53–61.
385 Green DM, Swets JA (1966) Signal detection theory and psychophysics. John Wiley and Sons
386   Inc.
387 Heisler JM, Morales J, Donegan JJ, Jett JD, Redus L, O'connor JC (2015) The attentional set
388   shifting task: A measure of cognitive flexibility in mice. J Vis Exp:2–7.
389 Hyman JM, Ma L, Balaguer-Ballester E, Durstewitz D, Seamans JK (2012) Contextual encoding
390   by ensembles of medial prefrontal cortex neurons. Proc Natl Acad Sci U S A 109:5086–
391   5091.
392 Jercog D, Winke N, Sung K, Fernandez MM, Francioni C, Rajot D, Courtin J, Chaudun F,
393   Jercog PE, Valerio S, Herry C (2021) Dynamical prefrontal population coding during
394   defensive behaviours. Nature Available at: http://www.ncbi.nlm.nih.gov/pubmed/34262175.
395 Ji G, Neugebauer V (2012) Modulation of medial prefrontal cortical activity using in vivo
396   recordings and optogenetics. Mol Brain 5:1–10.
397 Kim H, Ährlund-Richter S, Wang X, Deisseroth K, Carlén M (2016) Prefrontal Parvalbumin
398   Neurons in Control of Attention. Cell 164:208–218.
399 Lapiz-Bluhm MDS, Bondi CO, Doyen J, Rodriguez GA, Bédard-Arana T, Morilak DA (2008)
400   Behavioural assays to model cognitive and affective dimensions of depression and anxiety
401   in rats. J Neuroendocrinol 20:1115–1137.
402 Le Merre P, Ährlund-Richter S, Carlén M (2021) The mouse prefrontal cortex: Unity in diversity.
403   Neuron:1–20 Available at: https://linkinghub.elsevier.com/retrieve/pii/S0896627321002051.
404 Liston C, Miller MM, Goldwater DS, Radley JJ, Rocher AB, Hof PR, Morrison JH, McEwen BS
405   (2006) Stress-Induced Alterations in Prefrontal Cortical Dendritic Morphology Predict
406   Selective Impairments in Perceptual Attentional Set-Shifting. J Neurosci 26:7870–7874

407   Available at: http://www.jneurosci.org/cgi/doi/10.1523/JNEUROSCI.1184-06.2006.
408 Luk CH, Wallis JD (2009) Dynamic encoding of responses and outcomes by neurons in medial
409   prefrontal cortex. J Neurosci 29:7526–7539.
410 Mackintosh NJ (1975) A theory of attention: Variations in the associability of stimuli with
411   reinforcement. Psychol Rev 82:276–298.
412 Mansouri FA, Matsumoto K, Tanaka K (2006) Prefrontal cell activities related to monkeys'
413   success and failure in adapting to rule changes in a Wisconsin card sorting test analog. J
414   Neurosci 26:2745–2756.
415 Mansouri FA, Tanaka K, Buckley MJ (2009) Conflict-induced behavioural adjustment: A clue to
416   the executive functions of the prefrontal cortex. Nat Rev Neurosci 10:141–152.
417 Mante V, Sussillo D, Shenoy K V, Newsome WT (2013) Context-dependent computation by
418   recurrent dynamics in prefrontal cortex. Nature 503:78–84 Available at:
419   http://www.ncbi.nlm.nih.gov/pubmed/24201281 [Accessed February 19, 2014].
420 Markowitz JE, Gillis WF, Jay M, Wood J, Harris RW, Cieszkowski R, Scott R, Brann D, Koveal
421   D, Kula T, Weinreb C, Osman MAM, Pinto SR, Uchida N, Linderman SW, Sabatini BL,
422   Datta SR (2023) Spontaneous behaviour is structured by reinforcement without explicit
423   reward. Nature Available at: https://www.nature.com/articles/s41586-022-05611-2.
424 McAlonan K, Brown VJ (2003) Orbital prefrontal cortex mediates reversal learning and not
425   attentional set shifting in the rat. Behav Brain Res 146:97–103.
426 Megemont M, McBurney-Lin J, Yang H (2022) Pupil diameter is not an accurate real-time
427   readout of locus coeruleus activity. Elife 11:1–17 Available at:
428   https://elifesciences.org/articles/70510.
429 Megemont M, Tortorelli LS, McBurney-Lin J, Cohen JY, O'Connor DH, Yang H (2024)
430   Simultaneous recordings of pupil size variation and locus coeruleus activity in mice. STAR
431   Protoc 5:102785 Available at: https://doi.org/10.1016/j.xpro.2023.102785.
432 Mesulam MM (1998) From sensation to cognition. Brain 121:1013–1052.
433 Meyers EM, Freedman DJ, Kreiman G, Miller EK, Poggio T (2008) Dynamic population coding
434   of category information in inferior temporal and prefrontal cortex. J Neurophysiol 100:1407–
435   1419 Available at: https://www.physiology.org/doi/10.1152/jn.90248.2008.
436 Miller EK (1999) The prefrontal cortex: Complex neural properties for complex behavior. Neuron
437   22:15–17.
438 Miller EK, Cohen JD (2001) An Integrative Theory of Prefrontal Cortex Function. Annu Rev
439   Neurosci 24:167–202 Available at:
440   http://www.annualreviews.org/doi/10.1146/annurev.neuro.24.1.167.
441 Milner B (1963) Effects of Different Brain Lesions on Card Sorting. Arch Neurol 9:90 Available
442   at:
443   http://archneur.jamanetwork.com/article.aspx?doi=10.1001/archneur.1963.0046007010001
444   0.
445 Monchi O, Petrides M, Petre V, Worsley K, Dagher A (2001) Wisconsin card sorting revisited:
446   Distinct neural circuits participating in different stages of the task identified by event-related
447   functional magnetic resonance imaging. J Neurosci 21:7733–7741.
448 Musall S, Kaufman MT, Juavinett AL, Gluf S, Churchland AK (2019) Single-trial neural dynamics
449   are dominated by richly varied movements. Nat Neurosci 22:1677–1686 Available at:
450   http://dx.doi.org/10.1038/s41593-019-0502-4.
451 Nigro M, Tortorelli LS, Dinh K, Garad M, Zlebnik NE, Yang H (2023) Prefrontal dynamics and
452   encoding of flexible rule switching. bioRxiv.
453 Norman KJ et al. (2021) Post-error recruitment of frontal sensory cortical projections promotes
454   attention in mice. Neuron 109:1202-1213.e5 Available at:
455   https://doi.org/10.1016/j.neuron.2021.02.001.
456 Owen AM, Roberts AC, Polkey CE, Sahakian BJ, Robbins TW (1991) Extra-dimensional versus
457   intra-dimensional set shifting performance following frontal lobe excisions, temporal lobe

458   excisions or amygdalo-hippocampectomy in man. Neuropsychologia 29:993–1006.

459   Parker PRL, Brown MA, Smear MC, Niell CM (2020) Movement-Related Signals in Sensory
460   Areas: Roles in Natural Behavior. Trends Neurosci 43:581–595 Available at:
461   https://doi.org/10.1016/j.tins.2020.05.005.

462   Pi H-J, Hangya B, Kvitsiani D, Sanders JI, Huang ZJ, Kepecs A (2013) Cortical interneurons
463   that specialize in disinhibitory control. Nature Available at:
464   http://www.nature.com/doifinder/10.1038/nature12676 [Accessed October 6, 2013].

465   Pinto L, Dan Y (2015) Cell-Type-Specific Activity in Prefrontal Cortex during Goal-Directed
466   Behavior. Neuron 87:437–450 Available at: http://dx.doi.org/10.1016/j.neuron.2015.06.021.

467   Ragozzino ME (2007) The contribution of the medial prefrontal cortex, orbitofrontal cortex, and
468   dorsomedial striatum to behavioral flexibility. Ann N Y Acad Sci 1121:355–375.

469   Redish AD (2014) MClust Spike sorting toolbox Documentation for version 4.4. Available at:
470   https://redishlab.umn.edu/sites/redishlab.neuroscience.umn.edu/files/2021-04/MClust-4-4
471   documentation.pdf.

472   Reinert S, Hübener M, Bonhoeffer T, Goltstein PM (2021) Mouse prefrontal cortex represents
473   learned rules for categorization. Nature 593:411–417 Available at:
474   http://www.nature.com/articles/s41586-021-03452-z.

475   Rich EL, Shapiro M (2009) Rat prefrontal cortical neurons selectively code strategy switches. J
476   Neurosci 29:7208–7219.

477   Richman EB, Ticea N, Allen WE, Deisseroth K, Luo L (2023) Neural landscape diffusion
478   resolves conflicts between needs across time. Nature 623:571–579 Available at:
479   https://www.nature.com/articles/s41586-023-06715-z.

480   Ridderinkhof KR (2004) The Role of the Medial Frontal Cortex in Cognitive Control. Science
481   (80-) 306:443–447 Available at:
482   https://www.sciencemag.org/lookup/doi/10.1126/science.1100301.

483   Rigotti M, Barak O, Warden MR, Wang XJ, Daw ND, Miller EK, Fusi S (2013) The importance of
484   mixed selectivity in complex cognitive tasks. Nature 497:585–590.

485   Rikhye R V., Gilra A, Halassa MM (2018) Thalamic regulation of switching between cortical
486   representations enables cognitive flexibility. Nat Neurosci 21:1753–1763 Available at:
487   http://dx.doi.org/10.1038/s41593-018-0269-z.

488   Roberts AC, Robbins TW, Everitt BJ (1988) The Effects of Intradimensional and
489   Extradimensional Shifts on Visual Discrimination Learning in Humans and Non-human
490   Primates. Q J Exp Psychol Sect B 40:321–341.

491   Rodgers CC, DeWeese MR (2014) Neural correlates of task switching in prefrontal cortex and
492   primary auditory cortex in a novel stimulus selection task for rodents. Neuron 82:1157–
493   1170 Available at: http://dx.doi.org/10.1016/j.neuron.2014.04.031.

494   Rubenstein JLR, Merzenich MM (2003) Model of autism: increased ratio of excitation/inhibition
495   in key neural systems. Genes Brain Behav 2:255–267.

496   Rushworth MFS, Behrens TEJ (2008) Choice, uncertainty and value in prefrontal and cingulate
497   cortex. Nat Neurosci 11:389–397.

498   Siniscalchi MJ, Phoumthipphavong V, Ali F, Lozano M, Kwan AC (2016) Fast and slow
499   transitions in frontal ensemble activity during flexible sensorimotor behavior. Nat Neurosci
500   Available at: http://www.nature.com/doifinder/10.1038/nn.4342.

501   Sleezer BJ, Castagno MD, Hayden BY (2016) Rule encoding in orbitofrontal cortex and striatum
502   guides selection. J Neurosci 36:11223–11237.

503   Sleezer BJ, LoConte GA, Castagno MD, Hayden BY (2017) Neuronal responses support a role
504   for orbitofrontal cortex in cognitive set reconfiguration. Eur J Neurosci 45:940–951.

505   Snyder K, Wang WW, Han R, McFadden K, Valentino RJ (2012) Corticotropin-releasing factor
506   in the norepinephrine nucleus, locus coeruleus, facilitates behavioral flexibility.
507   Neuropsychopharmacology 37:520–530 Available at:
508   http://dx.doi.org/10.1038/npp.2011.218.

509   Sohal VS, Rubenstein JLR (2019) Excitation-inhibition balance as a framework for investigating
510   mechanisms in neuropsychiatric disorders. Mol Psychiatry 24:1248–1257 Available at:
511   http://dx.doi.org/10.1038/s41380-019-0426-0.
512   Spellman T, Svei M, Kaminsky J, Manzano-Nieves G, Liston C (2021) Prefrontal deep
513   projection neurons enable cognitive flexibility via persistent feedback monitoring. Cell
514   184:2750-2766.e17 Available at: https://doi.org/10.1016/j.cell.2021.03.047.
515   Steinmetz NA, Zatka-Haas P, Carandini M, Harris KD (2019) Distributed coding of choice,
516   action, and engagement across the mouse brain. Nature in press Available at:
517   http://dx.doi.org/10.1038/s41586-019-1787-x.
518   Stringer C, Pachitariu M, Steinmetz N, Reddy CB, Carandini M, Harris KD (2019) Spontaneous
519   behaviors drive multidimensional, brainwide activity. Science (80-) 364.
520   Tye KM, Miller EK, Taschbach FH, Benna MK, Rigotti M (2024) Mixed selectivity : Cellular
521   computations for complexity. Neuron:1–15 Available at:
522   https://doi.org/10.1016/j.neuron.2024.04.017.
523   Uddin LQ (2021) Cognitive and behavioural flexibility: neural mechanisms and clinical
524   considerations. Nat Rev Neurosci Available at: http://dx.doi.org/10.1038/s41583-021-
525   00428-w.
526   Wallis JD, Anderson KC, Miller EK (2001) Single neurons in prefrontal cortex encode abstract
527   rules. Nature 411:953–956 Available at: http://www.nature.com/articles/35082081.
528   Wiltschko AB, Johnson MJ, Iurilli G, Peterson RE, Katon JM, Pashkovski SL, Abraira VE,
529   Adams RP, Datta SR (2015) Mapping Sub-Second Structure in Mouse Behavior. Neuron
530   88:1121–1135 Available at: http://dx.doi.org/10.1016/j.neuron.2015.11.031.
531   Young JW, Powell SB, Geyer MA, Jeste D V., Risbrough VB (2010) The mouse attentional-set-
532   shifting task: A method for assaying successful cognitive aging? Cogn Affect Behav
533   Neurosci 10:243–251 Available at: http://link.springer.com/10.3758/CABN.10.2.243.
534   Zagha E, Erlich JC, Lee S, Lur G, O'Connor DH, Steinmetz NA, Stringer C, Yang H (2022) The
535   Importance of Accounting for Movement When Relating Neuronal Activity to Sensory and
536   Cognitive Processes. J Neurosci 42:1375–1382 Available at:
537   https://www.jneurosci.org/lookup/doi/10.1523/JNEUROSCI.1919-21.2021.
538   Zhou J, Jia C, Montesinos-Cartagena M, Gardner MPH, Zong W, Schoenbaum G (2021)
539   Evolving schema representations in orbitofrontal ensembles during learning. Nature
540   590:606–611 Available at: http://dx.doi.org/10.1038/s41586-020-03061-2.

541
542
543
544
545
546
547
548
549
550
551
552
553
554
555
556
557
558
559

Materials and Methods

All procedures were performed in accordance with protocols approved by UC Riverside Animal Care and Use Committee (#20190031). Ten C57BL/6 mice of 8-12 weeks and mixed sex were used in this study. Procedures for microdrive construction and recording were similar to our previous work (Megemont et al., 2022, 2024). Briefly, the implants were custom microdrives with eight tetrodes, each consisting of four nichrome wires (200–300 kΩ). The microdrive was implanted through a ~1 mm diameter craniotomy targeting the left mPFC (prelimbic area, 1.9-2.2 mm rostrocaudal and 0-0.5 mm mediolateral relative to bregma and 1 mm dorsoventral relative to brain surface). The microdrive was advanced in steps of 100 μm each day until reaching the recording depth of 1.4-1.6 mm. At the end of the experiment, an electrolytic lesion (100 μA, 20 s) was made prior to transcardial perfusion. Perfusions were done first with PBS followed by 4% PFA. The brain was sliced at 100 μm coronal sections to confirm the recording site.

Mice were singly housed after tetrode implant and allowed 2-3 days of recovery. Mice were then food restricted (80-85% of initial weight) and handled by the experimenter for 5-7 days. Next, mice were acclimated to the behavioral box (22 x 33 cm) and experimental setup for 1-2 days, followed by a brief training session to stimulate the innate burrowing/digging behavior to retrieve food reward from the ramekins. Two ramekins were placed at two corners of the behavioral box, both containing 25 mg of cheerios. Throughout the training session the reward was gradually buried in clean home cage bedding. In each trial mice were allowed 3-4 minutes to explore. Mice were considered well trained once they can consistently dig and retrieve the reward from both locations for 15-20 trials.

To assess flexible decision-making in freely moving mice, we adopted the 5-stage testing paradigm of the attentional set-shifting task (Liston et al., 2006; Snyder et al., 2012), consisting of the following stages: 1) simple discrimination (SD), in which animals choose between two digging medium associated with distinct textures (first stimulus dimension), only one of the two stimuli predicts food reward; 2) compound discrimination (CD), in which two odor cues (second stimulus dimension) are explicitly introduced. Each odor cue is randomly paired with a digging medium in every trial, but the reward is still predicted as in SD; 3) intra-dimensional reversal (REV), which preserves the task-relevant dimension (digging medium) but swaps cue contingencies; 4) intra-dimensional shift (IDS), which preserves the task-relevant dimension (digging medium), but replaces all four cues with novel ones (a new digging medium predicts reward); 5) extra-dimensional shift (EDS), which swaps the previous task-relevant and task-irrelevant dimensions with all cues replaced (a new odor cue predicts reward). All stages were performed within a single day, lasting 3-4 hours. In each trial, the ramekin associated with the relevant stimulus contained a retrievable reward. To avoid the possibility that mice used food odor cues to solve the task, the other ramekin contained a non-retrievable reward (trapped under a mesh wire at the bottom). The two ramekins were placed randomly in the two corners every trial. Between trials, mice were confined to the other side of the behavioral box (opposite to the ramekins) with a divider inserted ('waiting zone', Fig. S1), and had free access to water. Each trial started by removing the divider, and mice were allowed to make a decision (digging one ramekin) within 3 minutes. If no digging was performed within 3 minutes, the trial was scored as a null trial. Once mice started digging, the other ramekin was immediately removed from the behavioral box. If mice dug the correct ramekin to retrieve the reward (correct trial), a new trial would start once the reward was consumed. If mice dug the wrong ramekin embedded with the non-retrievable reward (incorrect trial), they would have a 1-minute timeout and a new trial would start.

A CCD camera (Basler acA1300-200um) was set above the behavioral box to capture the top-down view of mouse movements at 10 or 20 Hz, controlled by Pylon software. Video and

611 electrophysiology recordings were synchronized via a common TTL pulse train (Arduino).
612 Behavioral annotations were done manually post hoc.
613
614 Electrophysiology recordings were acquired at 20 kHz and hardware-filtered between 0.1-10 kHz
615 (Intan Technologies). Signals were bandpass filtered between 300-6000 Hz and spikes were
616 detected using a threshold of 4-8 standard deviations. The timestamp of the peak of each detected
617 spike, as well as a 1.6 ms waveform centered at the peak, was extracted from each channel for
618 offline spike sorting using MClust (Redish, 2014). Putatively duplicated units (peak correlation
619 coefficient > 0.5 and 0 ms peak lag between spike rasters) were removed from further analysis.
620 A recording session typically yielded 6-15 single units. A total of 161 single units were included in
621 the analyses (inter-cluster distances > 20, cluster quality measure L_{ratio} < 0.05). Cell type
622 classification was based on trough to peak, full width at half maximum (FWHM) and baseline firing
623 rate. Specifically, putative regular-spiking pyramidal neurons are identified by trough to peak >
624 0.5 ms and baseline firing rate < 10 Hz. Putative fast-spiking interneurons are identified by trough
625 to peak < 0.5 ms and baseline firing rate > 10 Hz. The remaining units are considered unidentified.
626
627 In order to classify neuronal representations of different task-related variables, we performed
628 Receiver-Operating-Characteristic (ROC) analysis on the firing rate of each unit for stimulus
629 dimension, previous trial outcome and current trial choice separately. Dimension representation
630 was defined as significant spiking responses between the odor-relevant stage (EDS) and
631 combined digging medium-relevant stages (CD, REV and IDS) during ITI (-5 to 0 s from trial start)
632 of the last 6 correct trials; a neuron was labeled 'context+' with the area under curve (AUC) > 0.5
633 and p < 0.05, conversely 'context-' neuron was defined with AUC < 0.5 and p < 0.05. Similar
634 analysis was performed to classify outcome encoding in individual task stages, comparing spiking
635 activity during ITI following correct trials against following incorrect trials. Removing the last 4
636 correct trials to better balance the number of correct and incorrect trials did not affect this analysis
637 (data not shown). Choice classification was performed during a time window immediately prior to
638 digging (-2 to 0 s from digging), comparing spiking activity preceding correct choices against
639 preceding incorrect choices.
640
641 In order to classify neuronal representations of different task-related variables, we performed
642 Receiver-Operating-Characteristic (ROC) analysis on the firing rate of each unit for stimulus
643 dimension, previous trial outcome and current trial choice separately. Context representation was
644 defined as significant spiking responses between the odor-relevant stage (EDS) and combined
645 digging medium-relevant stages (CD, REV and IDS) during ITI (-5 to 0 s from trial start) of the last
646 6 correct trials; a neuron was labeled 'context+' with the area under curve (AUC) > 0.5 and p <
647 0.05, conversely 'context-' neuron was defined with AUC < 0.5 and p < 0.05. Similar analysis was
648 performed to classify outcome encoding in individual task stages, comparing spiking activity
649 during ITI following correct trials against following incorrect trials. Outcome encoding analysis was
650 robust by removing the last 4 correct trials to better balance the number of correct and incorrect.
651 Choice classification was performed during a time window immediately prior to digging (-2 to 0 s
652 from digging) on each trial, comparing spiking activity preceding correct choices against preceding
653 incorrect choices.
654
655 To assess the impact of different task-related variables on neuronal activity, a multilinear
656 regression analysis was performed on the firing rate of each neuron (MATLAB function 'fitglm').
657 Categorical regressors were context (odor - 1, digging medium - 0), outcome of previous trial
658 (previous correct - 1, previous incorrect - 0), and choice of current trial (correct - 1, incorrect - 0).
659 In Fig. S3, all trials (including incorrect trials) in CD, REV, IDS and EDS were pooled to estimate
660 the coefficients. Model performance (fraction of variance explained, R^2) of the complete model
661 and the null model was compared using a permutation test: R^2 values from the complete and null

662 models were pooled, and then randomly assigned to two groups. The reported P values
663 represented the proportion of iterations where the mean R^2 difference between the two
664 permutated groups exceeded the observed difference from 1000 iterations. Complete model R^2
665 vs. null model R2, for Fig. S3 context+ neurons: 0.13 ± 0.028 vs. -0.0020 ± 0.0025, $p < 0.001$;
666 context- neurons: 0.14 ± 0.021 vs. $-9.6e-4 \pm 0.0028$, $p < 0.001$. In Fig. 5, 6 and Fig. S7-9, we
667 estimated the coefficients of context, outcome, and choice by training and testing our model on
668 data from CD, REV, IDS, and EDS stages. To estimate context coefficients, we pooled 80% of
669 the trials (including incorrect trials) from all four stages for training and used the remaining 20%
670 to test the model's predictive performance on firing rates. Similarly, for estimating outcome and
671 choice coefficients, we used 80% of the trials from each individual stage for training and the
672 remaining 20% for testing. The models were evaluated using 5-fold cross-validation. To assess
673 the model's performance in predicting neuronal firing rates, we calculated the root mean square
674 error (RMSE) for each temporal window. The RMSE values for choice and outcome in Fig. 5 and
675 S7-8 are as follows: $T1:1.26\pm0.13$; $T2:1.38\pm0.13$; $T3:1.63\pm0.19$; $T4:1.64\pm0.19$. For context:
676 $T1:0.89\pm0.1$; $T2:0.91\pm0.11$; $T3:1.01\pm 0.1$; $T4:1.01\pm0.13$. The RMSE values for choice and
677 outcome in Fig. 6 and S9: $T1:2.15\pm0.24$; $T2:1.87\pm0.21$; $T3:2.23\pm0.26$; $T4:1.92\pm0.26$. Additionally,
678 we calculated the Akaike Information Criterion (AIC) for the null model and compared it with the
679 complete model. The comparison showed a significant difference between the complete model
680 and the null model (complete model AIC: 59.45 ± 0.4 vs. null model AIC: 62.15 ± 0.44, p-value =
681 0.007). Similarly, for the context-specific model, there was a significant difference (context
682 complete model AIC: 161.81 ± 2.04 vs. context null model AIC: 164.33 ± 2, p-value = 0.012).
683
684 For decoding analysis, we trained a linear multiclass error-correcting output codes (ECOC) model
685 using support vector machine (SVM) binary learner and one-versus-one coding design (MATLAB
686 function 'fitcecoc'). We then used the MATLAB function 'predict' to examine decoding accuracy.
687 For context decoding (Fig. 2), we used the last six correct trials in each stage (CD to EDS) to
688 assess model prediction. For outcome and choice decoding (Fig. 3, 4), we used all trials in EDS
689 to assess model prediction. Decoding analysis was performed using subsets of neurons (i.e.,
690 context-encoding, outcome-encoding, etc.) from individual recordings and comparisons were
691 made between each recording and shuffled model. Due to relatively small number of trials in this
692 task (c.f. Fig. 1B), we did not split the dataset into a training set and a testing set to examine
693 decoding capacity. Instead, we shuffled class labels to establish chance level decoding accuracy.
694 We note that chance level decoding probability may not be at 50%, as the shuffled model typically
695 generated a prediction of uniform 0 or 1 states for all trials.
696
697 All data were presented as mean ± s.e.m. unless otherwise noted. Statistical tests were two-tailed
698 signed rank for paired comparisons, and repeated-measure ANOVA for multiple comparisons
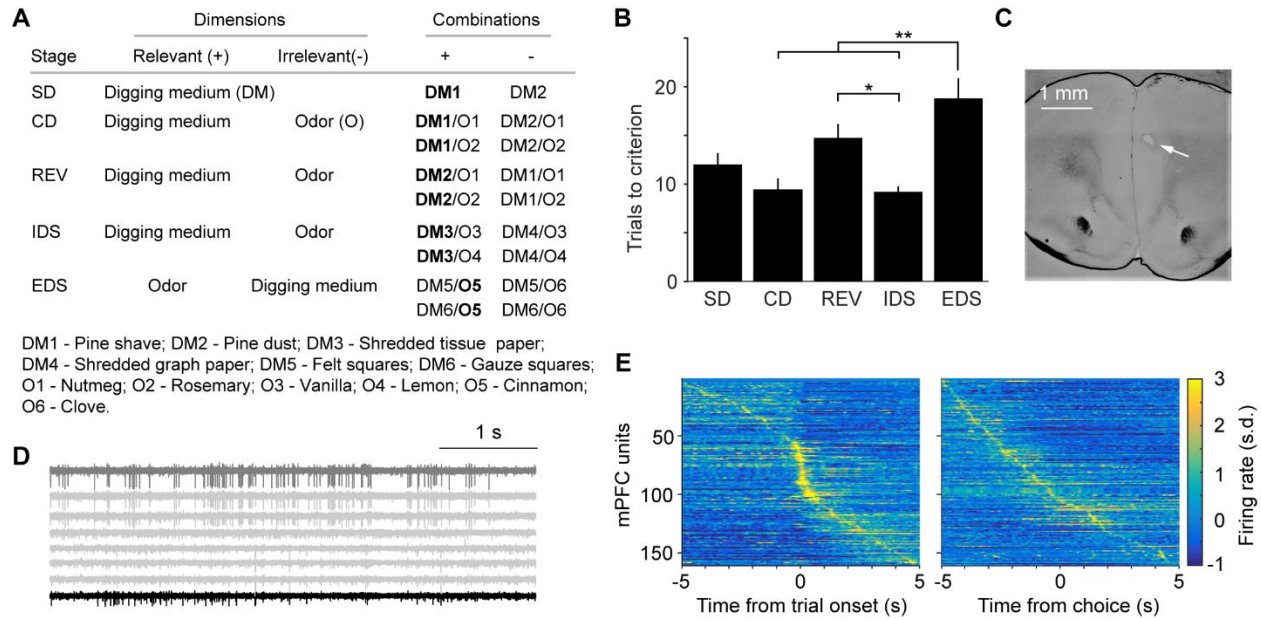699 unless otherwise noted.

Figure 1. Tetrode recording in the mPFC during AST.

(A) Test structure of AST.

(B) Task performance (total number of trials to criterion) varied across stages. Repeated-measure ANOVA, $F_{(4, 60)} = 8.6$, $p = 1.5e-5$, $n = 15$. Post hoc Tukey-Kramer tests revealed that mice took more trials to complete REV and EDS stages. REV vs. IDS, $p = 0.018$; EDS vs. CD, $p = 0.0038$; EDS vs. IDS, $p = 0.0052$. All other paired comparisons were not significantly different.

(C) Coronal brain section showing an electrolytic lesion marking the recording site (arrow) in the prelimbic region.

(D) Eight example traces from a 32-channel tetrode recording in the mPFC during behavior.

(E) Example heat map of trial-averaged spiking activity (z-scored) of all 161 units during trial onset (left) and during correct choice (right, ± 5 s) in EDS.
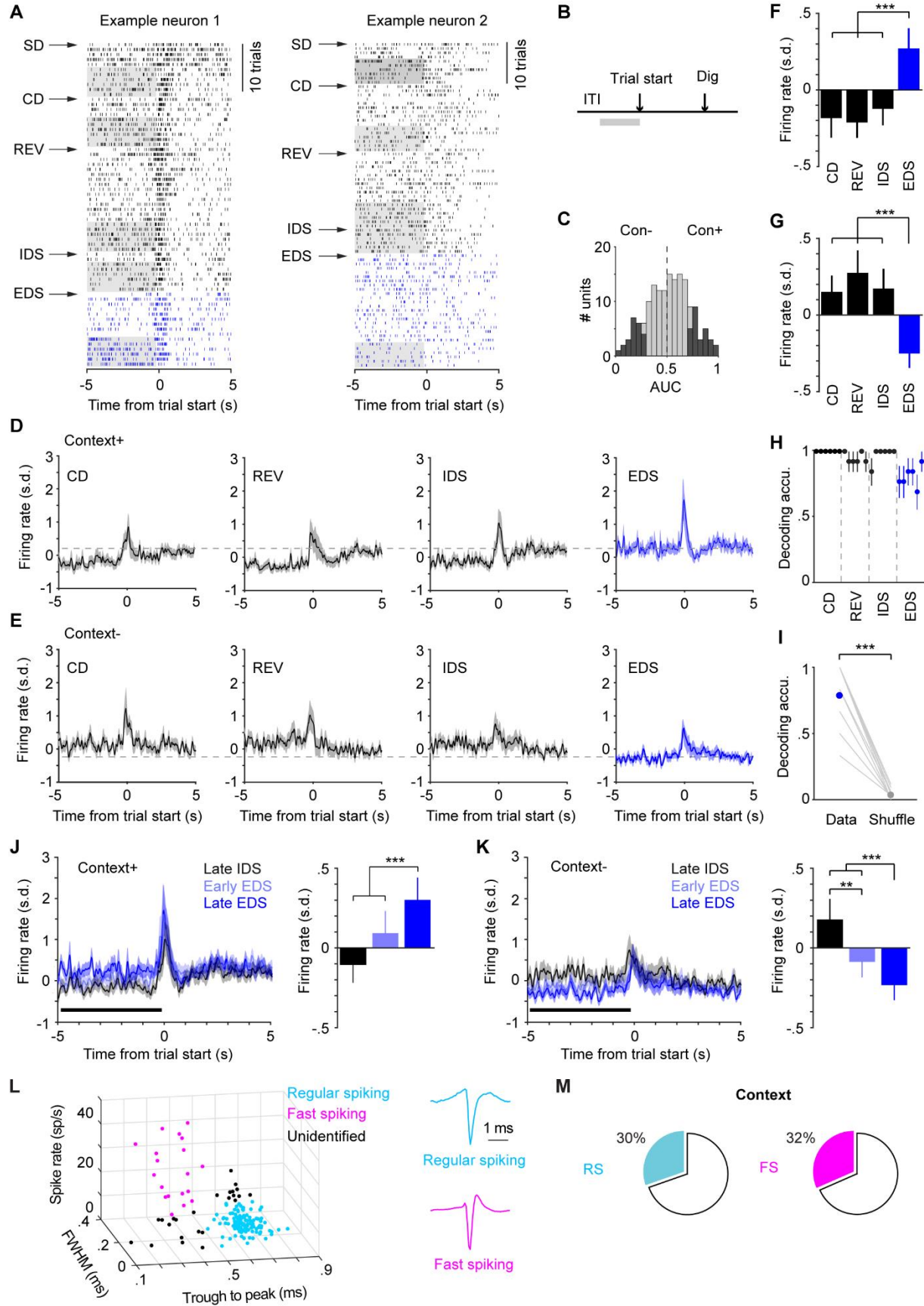
Figure 2. Task context encoding in the mPFC.

(A) Spike rasters from two example neurons showing enhanced (left) or suppressed (right) activity during intertrial intervals in the last 6 consecutive correct trials (grey area) in EDS compared with other stages. Ticks represent spikes.

(B) Illustration of the time window used to classify context encoding.

(C) Distribution of AUC values of context encoding for all neurons (light grey). Significantly modulated neurons ($p < 0.05$) were in dark.

(D) Group mean peri-event spike time histogram (PETH) of context+ neurons (n = 27) aligned to trial onset in stages CD through EDS. Mean firing rate during a 5-s window before trial start (black horizontal bar) is shown in E. Dashed line is to aid comparison.

(E) Group mean peri-event spike time histogram (PETH) of context- neurons (n = 23) aligned to trial onset in stages CD through EDS. Mean firing rate during a 5-s window before trial start (black horizontal bar) is shown in G.

(F) Context+ neurons showed significantly higher activity in EDS. Repeated-measures ANOVA, $F_{(3, 78)} = 16.1$, $p = 3.03e-8$, n = 27. Post hoc Tukey-Kramer tests: EDS vs. CD, $p = 2.1e-4$; EDS vs. REV, $p = 2.1e-6$; EDS vs. IDS, $p = 2.2e-4$. All other paired tests were not significant.

(G) Context- neurons showed significantly lower activity in EDS. Repeated-measures ANOVA, $F_{(3, 66)} = 15.14$, $p = 1.3e-7$, n = 23. Post hoc Tukey-Kramer tests: EDS vs. CD, $p = 6.4e-6$; EDS vs. REV, $p = 8.9e-6$; EDS vs. IDS, $p = 6.1e-5$. All other paired tests were not significant.

(H) Decoding of task context of the last six trials in stages CD through EDS (n = 15).

(I) Average decoding accuracy of last six trials in EDS for each recording (n = 15), compared with shuffled model (Data vs. Shuffle, $80.8 \pm 5.9\%$ vs. $2.6 \pm 0.9\%$, $p = 2.4e-4$).

(J) Left: Group mean PETH of context+ neurons aligned to trial onset from late IDS (black, last 6 correct trials), early EDS (light blue, all trials preceding last 6 correct trials), and late EDS (last six correct trials). Right: Mean firing rate during a 5-s window before trial start. Repeated-measures ANOVA, $F_{(2, 52)} = 13.1$, $p = 2.5e-5$, n = 27. Post hoc Tukey-Kramer tests: Late IDS vs. Early EDS, $p = 0.14$; Late IDS vs. Late EDS, $p = 1.1e-4$; Early EDS vs. Late EDS, $p = 2.4e-4$.

(K) Left: Group mean PETH of context- neurons aligned to trial onset from late IDS (black, last 6 correct trials), early EDS (light blue, all trials preceding last 6 correct trials), and late EDS (last six correct trials). Right: Mean firing rate during a 5-s window before trial start. Repeated-measures ANOVA, $F_{(2, 44)} = 20.9$, $p = 4.1e-7$, n = 23. Post hoc Tukey-Kramer tests: Late IDS vs. Early EDS, $p = 0.0095$; Late IDS vs. Late EDS, $p = 3.2e-5$; Early EDS vs. Late EDS, $p = 1.4e-5$.

(L) Classifying putative fast-spiking (magenta) and regular-spiking (cyan) neurons based on spike waveform features and spike rate.

(M) Similar proportions of RS and FS neurons encoded context. 34 out of 112 RS vs. 6 out of 19 FS, 30% vs. 32%, $p = 0.91$.
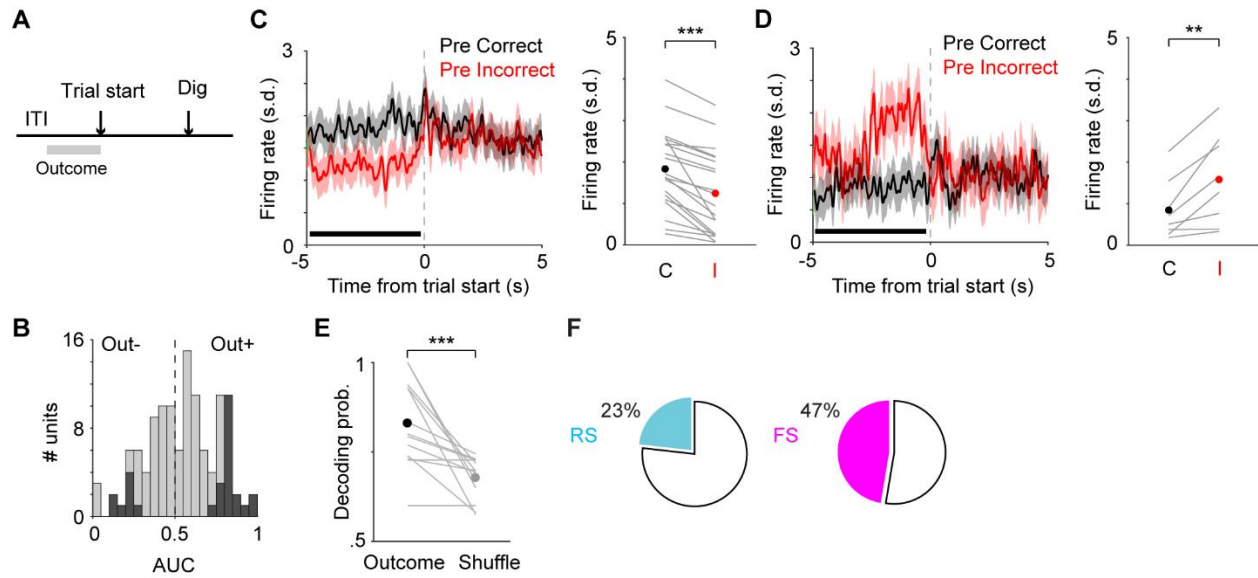
Figure 3. Trial outcome encoding in the mPFC.

(A) Illustration of the time window used to classify outcome encoding.

(B) Distribution of AUC values of outcome encoding for all neurons (light grey). Significantly modulated neurons (p < 0.05) were in dark.

(C) Left: Group mean PETH of outcome+ neurons in EDS (n = 23) aligned to trial onset when previous trials were correct (black) and incorrect (red). Right: Mean firing rate during a 5-s window before trial start when previous trials were correct (black) and incorrect (red). p = 2.7e-5. Lines: individual neurons. Dots: mean.

(D) Left: Group mean PETH of outcome- neurons in EDS (n = 13) aligned to trial onset when previous trials were correct (black) and incorrect (red). Right: Mean firing rate during a 5-s window before trial start when previous trials were correct (black) and incorrect (red). p = 2.4e-4. Lines: individual neurons. Dots: mean.

(E) Average outcome decoding accuracy of EDS for each recording (n = 15), compared with shuffled model (Outcome vs. Shuffle, 83.0 ± 3.4% vs. 66.9 ± 1.7%, p = 4.9e-4).

(F) Higher proportions of FS neurons encoded outcome. 26 out of 112 RS vs. 9 out of 19 FS, 23% vs. 47%, p = 0.028.
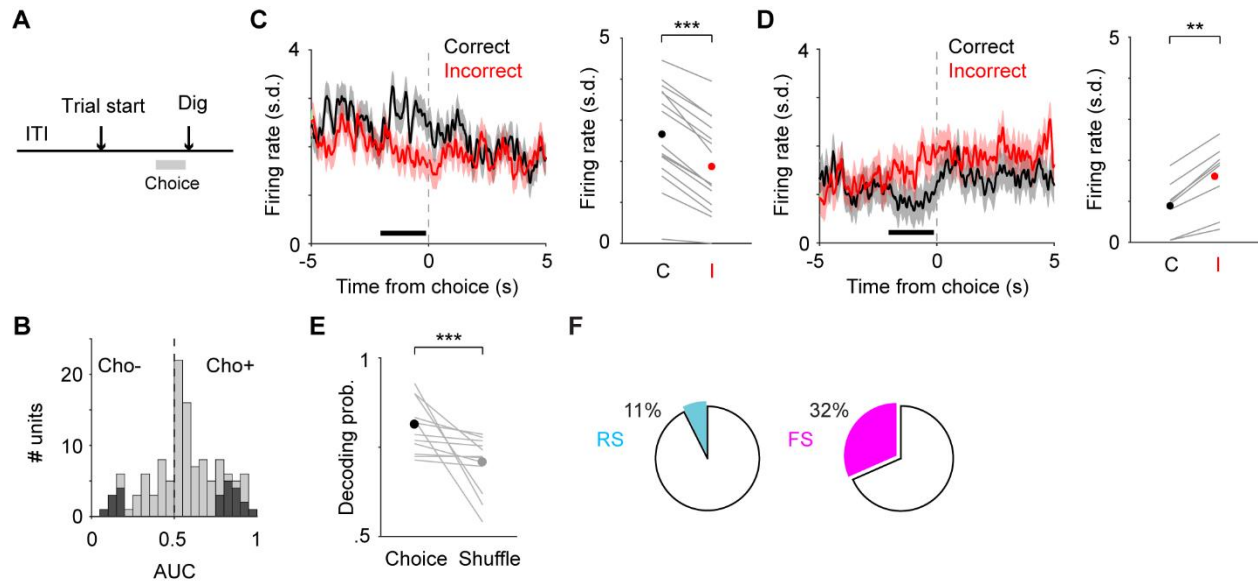
Figure 4. Choice encoding in the mPFC.

(A) Illustration of the time window used to classify choice encoding.

(B) Distribution of AUC values of choice encoding for all neurons (light grey). Significantly modulated neurons (p < 0.05) were in dark.

(C) Left: Group mean PETH of choice+ neurons in EDS (n = 13) aligned to trial onset when the upcoming choices of current trials were correct (black) and incorrect (red). Right: Mean firing rate during a 2-s window before digging when the upcoming choices of current trials were correct (black) and incorrect (red). p = 2.4e-4. Lines: individual neurons. Dots: mean.

(D) Left: Group mean PETH of choice- neurons in EDS (n = 10) aligned to trial onset when the upcoming choices of current trials were correct (black) and incorrect (red). Right: Mean firing rate during a 2-s window before digging when the upcoming choices of current trials were correct (black) and incorrect (red). p = 0.002. Lines: individual neurons. Dots: mean.

(E) Average choice decoding accuracy of EDS for each recording (n = 15), compared with shuffled model (Choice vs. Shuffle, 80.8 ± 2.1% vs. 70.6 ± 2.3%, p = 9.8e-4).

(F) Higher proportions of FS neurons encoded choice. 12 out of 112 RS vs. 6 out of 19 FS, 11% vs. 32%, p = 0.015.
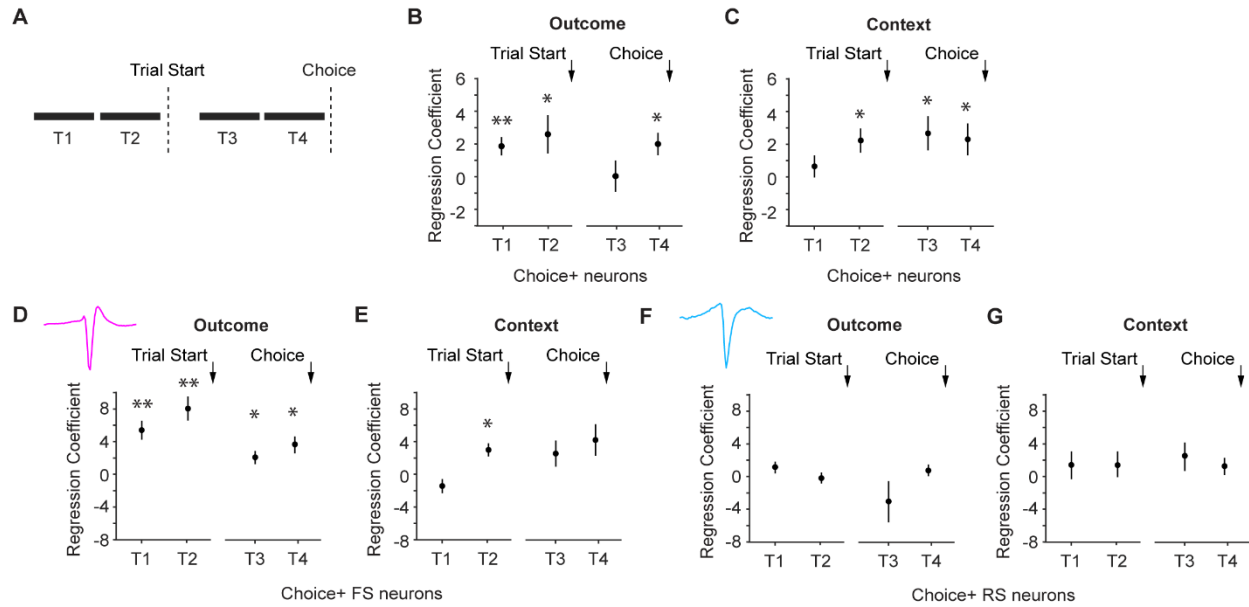
Figure 5. Context and outcome modulate choice-encoding neuronal activity in EDS

(A) Illustration of the four trial epochs. T1: -4 to -2 s from trial onset; T2: -2 to 0 s from trial onset; T3: -4 to -2 s from digging, T4: -2 to 0 s from digging;

(B) Regression coefficients of the outcome regressor for choice+ neurons (n = 13). Coefficients in T1, T2 and T4 were significantly different from 0. T1, p = 0.01; T2, p = 0.05; T3, p = 0.97; T4, p = 0.01.

(C) Regression coefficients of the context regressor for choice+ neurons (n = 13). Coefficients in T2, T3 and T4 were significantly different from 0. T1, p = 0.48; T2, p = 0.02; T3, p = 0.03; T4, p = 0.04.

(D) Regression coefficients of the outcome regressor for fast-spiking choice+ neurons in EDS (n = 5). Coefficients were significantly different from 0 in all epochs. T1, p = 0.009; T2, p = 0.005; T3, p = 0.038; T4, p = 0.025.

(E) Regression coefficients of the context regressor for fast-spiking choice+ neurons in EDS (n = 5). Coefficients in T2 were significantly different from 0. T1, p = 0.12; T2, p = 0.02; T3, p = 0.17; T4, p = 0.1.

(F) Regression coefficients of the outcome regressor for regular-spiking choice+ neurons (n = 5). Coefficients were not significantly different from 0 in any epochs. T1, p = 0.20; T2, p = 0.49; T3, p = 0.23; T4, p = 0.5.

(G) Regression coefficients of the context regressor for regular-spiking choice+ neurons in EDS (n = 5). Coefficients were not significantly different from 0 in any epochs. T1, p = 0.49; T2, p = 0.44; T3, p = 0.26; T4, p = 0.34. T test for all comparisons in Fig. 5.
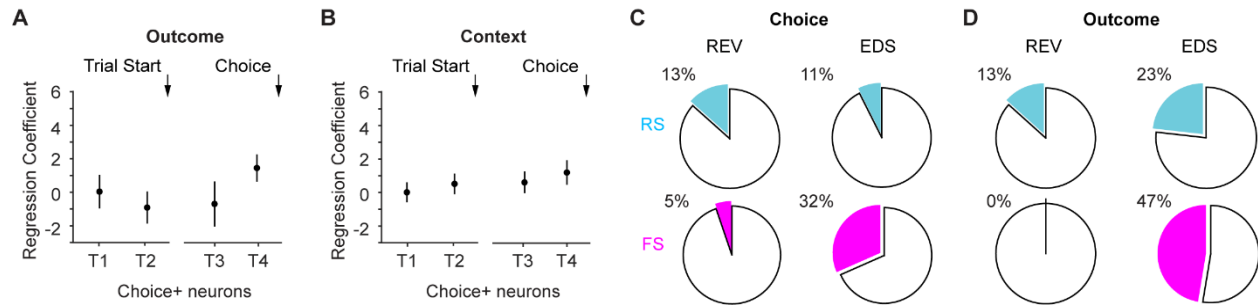
Figure 6. Context and outcome do not modulate choice-encoding neuronal activity in REV

(A) Regression coefficients of the outcome factor for choice+ neurons in REV (n = 13). Coefficients were not significantly different from 0 in any epochs. T1, p = 0.99; T2, p = 0.35; T3, p = 0.63; T4, p = 0.09.

(B) Regression coefficients of the context factor for choice+ neurons in REV (n = 13). Coefficients were not significantly different from 0 in any epochs. T1, p = 0.92; T2, p = 0.38; T3, p = 0.3; T4, p = 0.1.

(C) Comparison of the proportions of cell type-specific choice-encoding neurons in REV and EDS.

(D) Comparison of the proportions of cell type-specific outcome-encoding neurons in REV and EDS.